Acta Crystallographica Section A
Foundations of Crystallography
ISSN 0108-7673

Received 2 August 2010
Accepted 14 October 2010

Ab initio reconstruction of difference densities by charge flipping

Lukáš Palatinus,[a]* Frank Fleischer,[b] Phillip Pattison,[c,d] Thomas Weber[b] and Walter Steurer[b]

[a]Institute of Physics, Academy of Sciences of the Czech Republic, Na Slovance 2, 182 21 Prague, Czech Republic, [b]Laboratory of Crystallography, Department of Materials, ETH Zurich, Wolfgang-Pauli-Strasse 10, 8093 Zurich, Switzerland, [c]Ecole Polytechnique Fédérale de Lausanne, Laboratoire de Cristallographie, BSP, CH-1015 Lausanne, Switzerland, and [d]Swiss–Norwegian Beam Lines, ESRF, BP 220, F-38043 Grenoble, France. Correspondence e-mail: palat@fzu.cz

The charge-flipping algorithm in its band-flipping variant is capable of *ab initio* reconstructions of scattering densities with positive and negative values. It is shown that the method can be applied to reconstructions of difference electron densities of superstructures, *i.e.* densities obtained as a difference between the true scattering density and the average density over two or more subcells of the true structure. The amplitudes of reflections lying on the reciprocal lattice of the subcell are not required for the procedure. A series of examples shows applications of the method to the solution of superstructures in periodic crystals or quasicrystals as well as the application to *ab initio* solution of modulation of an incommensurately modulated structure from satellite reflections only and solution of a structure from a crystal twinned by reticular pseudomerohedry. The method is especially suited for solving pseudosymmetry problems occurring frequently in superstructures.

1. Introduction

Structure solution from X-ray or neutron diffraction data can be considered a mature field in many respects. Standard structure solution methods are powerful and can routinely solve structures with up to several hundred or even a few thousand independent atoms. However, special cases can still pose problems. One of the frequently occurring phenomena that complicate structure solution is pseudotranslation effects, or so-called superstructures. Superstructures can be described to a good approximation by a smaller unit cell, but the true structure has a larger unit cell (called supercell) with a volume that is an integer multiple of the small unit cell. The electron density in the individual subcells deviates only slightly from an average density obtained by averaging the density over the individual subcells. In reciprocal space the superstructure is characterized by the presence of two classes of reflections: strong main reflections containing information about the average density, and relatively weak superstructure reflections containing the information about the difference between the true and the average density. Probably the first systematic treatment of the problem was proposed by Buerger (1954) using the properties of a partial Patterson function. A detailed account of this method was presented by Takéuchi (1972).

The problem with superstructures lies in the often very small differences between the subcells, and the correspondingly weak intensities of the superstructure reflections. As a result, the assumptions underlying the statistical approaches of direct methods, namely the essentially random distribution of the atoms in the unit cell, are no longer fulfilled. The problem has been treated by different scaling of the main and superstructure reflections (Hauptman & Karle, 1959; Böhme, 1982; Beurskens *et al.*, 1990), but even with these approaches the problem remains difficult, and the difficulty increases with the multiplicity of the superstructure.

Rius *et al.* (1996) proposed an alternative method of solving superstructures by reconstructing directly the difference between the true density and the average density. Because the difference density contains both positive and negative peaks, the commonly used similarity between ρ and ρ^2 cannot be used. Rius *et al.* (1996) used instead the similarity between ρ and ρ^3, which preserves the sign of ρ. The resulting phase relationships thus contain only quartet and quintet invariants. This property makes the method computationally rather involved and applicable only to simple cases. Recently, Rius & Frontera (2008) proposed an improved approach based on the previously published S-FFT direct methods algorithm (Rius *et al.*, 2007).

Here we propose an alternative method to reconstruct directly the difference density using only the superstructure reflections. The method is based on the charge-flipping algorithm (Oszlányi & Sütő, 2004, 2005, 2008) in its band-flipping variant (Oszlányi & Sütő, 2007), which allows *ab initio* reconstructions of scattering densities with both positive and negative regions. In the original paper, the method was proposed for the reconstruction of neutron scattering densities

in the presence of atoms with negative scattering lengths. We show that the method can also be successfully applied to the solution of superstructures. In a series of case studies it is shown that the method is useful in the case of classical superstructures, but also in the structure solution of modulated structures, superstructures in quasicrystals and certain types of twins.

The formalism behind the reconstruction of difference densities and the method are described in §2. In the same section an overview of possible applications is presented. §3 contains a description of applications of the method to experimental data. The purpose of this section is not to work out a detailed structure analysis, but to demonstrate the ability of the presented method to obtain structural information in various cases. General observations, properties and limits of the method are then discussed in §4.

2. Theoretical

2.1. Average and difference density

Let ρ be the scattering density in the unit cell of a crystal structure. The unit cell is defined by three basis vectors $\mathbf{a}$, $\mathbf{b}$, $\mathbf{c}$. ρ can be calculated by Fourier transform of complex structure factors $F_{\mathbf{h}}$. Let us define a subcell of the unit cell defined by three vectors $\mathbf{a}_{\rm sub}$, $\mathbf{b}_{\rm sub}$, $\mathbf{c}_{\rm sub}$ such that

$$(\mathbf{a}, \mathbf{b}, \mathbf{c}) = (\mathbf{a}_{\rm sub}, \mathbf{b}_{\rm sub}, \mathbf{c}_{\rm sub})\mathbf{S}. \tag{1}$$

$\mathbf{S}$ is a matrix with integer elements, and its determinant gives the number $N_{\rm s}$ of subcells per one unit cell of the structure. Let the set $\{\mathbf{o}_i, i = 1, \ldots, N_{\rm s}\}$ be the lattice nodes of the subcells inside the unit cell. Vectors $\mathbf{o}_i$ can be expressed in the true unit cell by means of vectors $\mathbf{t}_i$ with integer components as

$$\mathbf{o}_i = \mathbf{S}^{-1}\mathbf{t}_i. \tag{2}$$

With the relationship between the subcell and the true cell defined, we can divide ρ into two parts: the average density, which is an average over the $N_{\rm s}$ subcells, and the difference between the true and average density:

$$\rho = \rho_{\rm av} + \rho_{\rm dif}. \tag{3}$$

The average density is defined as

$$\rho_{\rm av}(\mathbf{r}) = \frac{1}{N_{\rm s}}\sum_{i-1}^{N_{\rm s}} \rho(\mathbf{r} + \mathbf{o}_i). \tag{4}$$

By definition, $\rho_{\rm av}$ has the periodicity of the subcell. In the Fourier space this means that the Fourier coefficients of $\rho_{\rm av}$ will lie on the nodes of the reciprocal lattice spanned by vectors $\mathbf{a}^*_{\rm sub}, \mathbf{b}^*_{\rm sub}, \mathbf{c}^*_{\rm sub}$, which are obtained from $\mathbf{a}^*, \mathbf{b}^*, \mathbf{c}^*$ through the matrix $\mathbf{S}$:

$$\begin{pmatrix} \mathbf{a}^*_{\rm sub} \\ \mathbf{b}^*_{\rm sub} \\ \mathbf{c}^*_{\rm sub} \end{pmatrix} = \mathbf{S}\begin{pmatrix} \mathbf{a}^* \\ \mathbf{b}^* \\ \mathbf{c}^* \end{pmatrix}. \tag{5}$$

If $\mathbf{h}$ is a reciprocal-lattice vector of the true (small) reciprocal lattice, then $F_{\rm av}(\mathbf{h})$ is nonzero only if $\mathbf{h}^T\mathbf{S}^{-1}$ has integer components, and zero otherwise. Furthermore, we can write

$$\begin{aligned} F(\mathbf{h}) &= \int_V \rho(\mathbf{r}) \exp\left(2\pi i \mathbf{h}^T\mathbf{r}\right) {\rm d}V \\ &= \int_{V/N_{\rm s}} \sum_{i=1}^{N_{\rm s}} \rho(\mathbf{r} + \mathbf{o}_i) \exp\left[2\pi i \mathbf{h}^T(\mathbf{r} + \mathbf{o}_i)\right] {\rm d}V \\ &= \int_{V/N_{\rm s}} \exp\left(2\pi i \mathbf{h}^T\mathbf{r}\right) \sum_{i=1}^{N_{\rm s}} \rho(\mathbf{r} + \mathbf{o}_i) \exp\left(2\pi i \mathbf{h}^T\mathbf{S}^{-1}\mathbf{t}_i\right) {\rm d}V. \end{aligned} \tag{6}$$

The integration limit V represents an integration over the whole unit cell, while $V/N_{\rm s}$ represents integration over one subcell only. If $\mathbf{h}^T\mathbf{S}^{-1}$ is a vector with integer components, the exponential inside the sum on the last line of equation (6) equals 1, and, making use of equation (4), we can further write

$$\begin{aligned} F(\mathbf{h}) &= \int_{V/N_{\rm s}} \exp\left(2\pi i \mathbf{h}^T\mathbf{r}\right) \sum_{i=1}^{N_{\rm s}} \rho(\mathbf{r} + \mathbf{o}_i) {\rm d}V \\ &= \int_V \exp\left(2\pi i \mathbf{h}^T\mathbf{r}\right) \frac{1}{N_{\rm s}} \sum_{i=1}^{N_{\rm s}} \rho(\mathbf{r} + \mathbf{o}_i) {\rm d}V \\ &= \int_V \exp\left(2\pi i \mathbf{h}^T\mathbf{r}\right) \rho_{\rm av}(\mathbf{r}) {\rm d}V \\ &= F_{\rm av}(\mathbf{h}). \end{aligned} \tag{7}$$

As ρ is a sum of $\rho_{\rm av}$ and $\rho_{\rm dif}$, so are their Fourier spectra, and it thus follows that the Fourier components $F(\mathbf{h})$ are either fully determined by $\rho_{\rm av}$, or by $\rho_{\rm dif}$:

$$F(\mathbf{h}) = \begin{cases} F_{\rm av}(\mathbf{h}) & \text{if } \mathbf{h}^T\mathbf{S}^{-1} \text{ is integer,} \\ F_{\rm dif}(\mathbf{h}) & \text{otherwise.} \end{cases} \tag{8}$$

The amplitudes of the Fourier coefficients of $\rho_{\rm av}$ and $\rho_{\rm dif}$ are thus available from the diffraction experiment as two distinct classes of reflections. If the phases of $F_{\rm dif}$ can be found *ab initio* without using $F_{\rm av}$, the difference density $\rho_{\rm dif}$ can be reconstructed independently of $\rho_{\rm av}$. A method for reconstruction of $\rho_{\rm dif}$ based on the charge-flipping algorithm is described in §2.2.

The reason for the need for a special method for the reconstruction of $\rho_{\rm dif}$ is twofold. First, $\rho_{\rm dif}$ can contain both positive and negative values, and thus the classical approaches cannot be used as they rely on the positivity of the scattering density. Second, the shape of peaks in $\rho_{\rm dif}$ can be quite variable, and, depending on the nature of $\rho_{\rm av}$ and $\rho_{\rm dif}$, can deviate substantially from spherically symmetric peaks. As a result, the form factors of the peaks are not known, and normalization of $\rho_{\rm dif}$ becomes difficult. This problem can hamper solution of superstructures by classical direct methods (Beurskens & Bosman, 1982).

The ability to solve difference densities from a subset of reflection intensities has manifold applications. The obvious application is the solution of superstructures. In this case $F_{\rm av}$ is on average much stronger than $F_{\rm dif}$, and $\rho_{\rm dif}$ describes small variations between the density in the individual subcells, which are, in general, very similar. The experimental uncertainties on the much stronger $F_{\rm av}$ are often of the same order of magnitude as the amplitudes of $F_{\rm dif}$, and can obscure the superstructure features in the total density map. The direct

reconstruction of the difference density has the advantage of filtering out the major contribution to ρ from ρ_{av}, and providing direct insight into the superstructural features. Moreover, while the total density shows a pronounced pseudosymmetry, ρ_{dif} shows the true symmetry of the structure, which is then much more easily inferred. This possibility is illustrated in §§3.1 and 3.2. Superstructures do not occur only in ordinary periodic structures, but also in quasicrystals (QC). The structures of quasicrystals are described in higher-dimensional space (five-dimensional for decagonal and six-dimensional for icosahedral QCs). Despite the different dimensionality, the concept of superstructure reconstruction can also be applied to quasicrystals, as is illustrated in §3.5.

The problem of weak superstructure reflections is probably the most obvious case where the formalism introduced above applies. However, nowhere in the derivation of the formulas above was the assumption made that F_{av} is on average much stronger than F_{dif}. The method can thus also be applied to cases other than superstructures. A particularly attractive case is that of twinning by reticular merohedry. These twins have a twin index larger than one, and a reciprocal lattice exists that is a superlattice of both (or all) twin domains (see Nespolo & Ferraris, 2004, for a recent overview). In this case the reflections on this superlattice can be considered as F_{av}, and the remaining reflections as F_{dif}. The set of $|F_{av}|$ is not known from the experiment, because reflections from several twin domains overlap at these positions. This overlap can hamper the structure solution. On the other hand, the reflections not lying on the superlattice are separated, and thus the set of $|F_{dif}|$ is known for individual twin domains. As a result, the structure can be inferred by reconstructing the difference density from $|F_{dif}|$. An example of this case is documented in §3.3. A similar case is the problem of intergrowths of several polytypes. Several polytypes of the same compound have unit cells that are usually closely related, and if they are present in the same crystal, subsets of their reflections (called family reflections) overlap. Other reflections, however, remain separated (polytype reflections). The individual polytypic structures can be determined from polytype reflections only.

Another interesting case occurs if all F_{av} lie on a section of the reciprocal space. This case is contained in the formalism above, if one or two basis vectors of the subcell are allowed to have an infinitely small length, or, more generally, if one or two eigenvalues of the matrix **S** go to infinity. The section can be a plane (one infinite eigenvalue) or a line (two infinite eigenvalues). In such a case ρ_{av} is obtained by projecting ρ onto the plane or line of the section, and extending the projected density back along the projection directions. ρ_{dif} is then the difference between the true density and the extended projection. Applications of this concept to ordinary periodic structures are probably rather limited, because the number of reflections lying on the section is small compared to the total number of reflections, and even if they are not available for any reason, their absence would probably not prevent the structure solution. However, the situation is different in incommensurately modulated structures. These structures are described in higher-dimensional space (called superspace), and their reflections are indexed by more than three integers (Janssen *et al.*, 2007; van Smaalen, 2007). These structures can be described as an average three-dimensional periodic structure perturbed by an additional modulation, which is incommensurate with the periodicity of the average structure. In the superspace description the average structure is obtained as a projection of the total higher-dimensional structure onto the three-dimensional space. In reciprocal space the modulated structures are characterized by two sets of reflections. The so-called main reflections contain information about the average structure, and can be indexed with three integers. The so-called satellite reflections require four or more integer indices, and contain information about the modulation. Thus, the main reflections can be considered as F_{av} in the formalism above, and the satellite reflections correspond to F_{dif}. In the absence of the main reflections the information about the true structure can still be obtained by reconstructing the difference between the true higher-dimensional density and the average structure. The main reflections can be unavailable for at least two reasons. First, the modulated structures often exhibit twinning such that the main reflections of the twin domains overlap, but the satellites are separated. Second, the main reflections are usually much stronger than the satellites. If an experiment is optimized to collect the intensities of the satellites, most of the main reflections will probably be saturated. While it is certainly desirable in such a case to perform an additional experiment to collect the intensities of the main reflections, it can happen that such an experiment is not available, and then the present approach can provide at least some insight into the structure of the crystal from the partial data set.

2.2. Charge-flipping algorithm for densities without positivity constraint

Charge flipping (CF) is a dual-space iterative phasing method. It was published in 2004 (Oszlányi & Sütő, 2004), and further analysed and improved in a series of subsequent papers (Oszlányi & Sütő, 2005, 2007, 2008). It is based on a standard Fourier cycle, *i.e.* on alternating between the direct and reciprocal space, and applying modification to the trial scattering density in the former, and to the structure factors in the latter space. In this general principle it is not different from other methods alternating between the two spaces. What makes charge flipping specific is the type of the modifications. In reciprocal space the basic modification consists of a simple replacement of the structure-factor amplitudes by the experimental ones, and in direct space the density is modified by multiplying all density values below a certain small positive threshold δ by -1. The iteration is continued until convergence is detected, or until a prescribed number of cycles is reached. Charge flipping has been used in many applications since its publication. An application particularly relevant to this study is the solution of a pseudosymmetric structure by charge flipping (Oszlányi *et al.*, 2006), where it was demonstrated that the standard charge-flipping algorithm is already a

good tool for solving structures with translational pseudo-symmetry.

Because all negative density values are made positive by the charge-flipping modification, the basic algorithm is applicable only to positive densities. However, Oszlányi & Sütő (2007) have shown that by a simple variation of the density modification the method can be generalized to densities with both positive and negative values. The density modification in this so-called 'band-flipping' variant is multiplication by -1 of all density values between $-\delta$ and $+\delta$. Thus, large negative peaks remain preserved, and negative densities can develop. Oszlányi and Sütö show that the sparseness of the density is a sufficient condition for the algorithm to work, and that positivity is not strictly required, although it facilitates the solution in cases when it is applicable, as it is a stronger constraint than the sparseness alone.

The motivation for the development of the band-flipping variant of charge flipping was its ability to reconstruct directly the neutron scattering densities in the presence of atoms with negative scattering power. However, charge flipping neither requires normalization of input structure-factor amplitudes, nor does it use the atomic form factors in any manner, and therefore can be applied to the reconstruction of any density distribution under the condition that the distribution is sparse. The band-flipping algorithm can thus be directly applied to reconstruction of difference electron densities from subsets of structure-factor amplitudes, as derived in the previous section.

One of several outstanding properties of the charge-flipping algorithm is the fact that it does not require the *a priori* knowledge of symmetry for the phasing process. As a result the density is retrieved in space group $P1$, and it is possible to derive the symmetry from the reconstructed density (Palatinus & van der Lee, 2008). If the structure is a superstructure, then it is frequently pseudosymmetric, and the symmetry determination directly from diffraction data can be difficult. If, however, only the difference density is reconstructed *ab initio*, the part with the higher symmetry is not present, and the difference density can be analysed for symmetry more easily.

It is an established fact that charge flipping alone provides only a relatively inaccurate approximation of the true electron density, and that further iteration steps with different density modification are needed to improve the phases (Oszlányi & Sütő, 2008; Palatinus & Chapuis, 2007; Fleischer *et al.*, 2010). Fleischer *et al.* (2010) demonstrated quantitatively that the low-density elimination (LDE) method (Shiono & Woolfson, 1992) is a suitable iteration method to improve substantially the solution obtained by charge flipping. The only difference between the basic CF algorithm and LDE is the density modification step. For LDE the modification consists of a simple resetting of all negative density values to zero. This approach cannot be used for densities with negative values. Instead, a 'band density elimination' approach must be used, where all density values between $-\delta_{\rm LDE}$ and $+\delta_{\rm LDE}$ are set to zero. Although $\delta_{\rm LDE}$ can be, in general, different from $\delta_{\rm CF}$, and Oszlányi & Sütő (2008) propose, in a related context, to make it slightly larger than $\delta_{\rm CF}$, our experience shows that the precise value of $\delta_{\rm LDE}$ is not critical for the quality of the result, and using $\delta_{\rm CF}$ also for the LDE step is appropriate.

All calculations in the following sections were performed with the program *SUPERFLIP* (Palatinus & Chapuis, 2007). This program includes the possibility of applying the band-flipping algorithm and the low-density elimination including the band elimination variant. *SUPERFLIP* also contains an option for deriving the symmetry of the structure from the

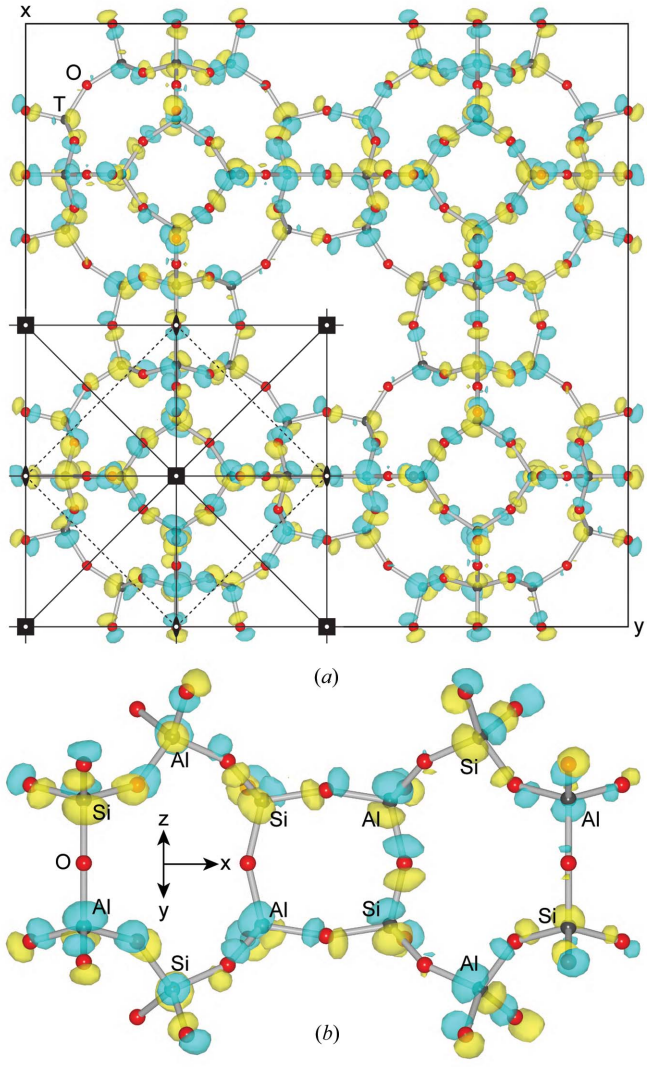

Figure 1
(*a*) (001) projection of the difference electron-density (ED) map of zeolite *A* (unit cell plotted in the range $0 \le z \le 0.5$). The ED map of the $2 \times 2 \times 2$ superstructure is superimposed with the average structure framework. Selected symmetry elements ([001] rotation axes and mirror planes parallel to [001]) of the average structure space group $Pm\bar{3}m$ are drawn for one subcell to illustrate symmetry breaking in the superstructure. The only preserved symmetry operation visible in this projection is the twofold axis in the centre of the image, and two antisymmetric diagonal mirror planes. (*b*) ⟨110⟩ projection of the asymmetric unit. The *T*-atom distribution between Al and Si was deduced from the position of the positive and negative peaks. Yellow corresponds to positive and turquoise to negative ED values. The threshold for the isosurface level is set to 20% of the ED maxima. This as well as other images of density isosurfaces were produced by the crystallographic three-dimensional visualization program *VESTA* (Momma & Izumi, 2008).

reconstructed density. It is capable of reconstructing densities in arbitrary dimensions, which makes it also suitable for dealing with modulated structures and quasicrystals.

3. Applications

3.1. Zeolite *A*

The Na-substituted zeolite *A* is one of the most studied zeolites. Its framework structure is of the LTA type [see Baerlocher & McCusker (2010) for an overview of zeolite framework types] and its idealized composition is $NaAlSiO_4$. The framework structure of zeolite *A* can be described to a good approximation in a cubic unit cell with a = 12.6 Å with symmetry $Pm\overline{3}m$ (Fig. 1*a*). However, ordering of the Si and Al atoms leads to doubling of the unit-cell dimensions in all three directions. The correct space group of the superstructure was the subject of a heated debate in the 1980s. While most investigators advocated the structure model with space group $Fm\overline{3}c$ with alternating SiO_4 and AlO_4 tetrahedra, denoted Si(4Al) (Smith & Pluth, 1981; Adams & Haselden, 1982; Gramlich-Meier & Gramlich, 1982, and references therein), several works appeared that advocated an alternative model denoted Si(3Al), where each Si tetrahedron is surrounded by three Al tetrahedra and one Si tetrahedron (Bursil *et al.*, 1981; Lippmaa *et al.*, 1981). The deviation of the structure from the small cell is quite small, because it is caused only by chemical ordering of Si and Al, and by the accompanying small shifts of the oxygen atoms due to the difference in the Si—O and Al—O bond lengths. To test the method described in this work, we decided to try to use it for reconstruction of the superstructure of Na-*A* zeolite. We used a single-crystal sample of zeolite *A* that serves as a test and calibration sample at the Swiss–Norwegian beamline at ESRF, Grenoble. The sample was prepared by the conventional synthetic method (Charnel, 1971). The data were collected with synchrotron radiation, wavelength λ = 0.7245 Å, T = 100 K to the resolution of $d_{\min}$ = 0.78 Å. All reflections could be indexed with a cubic cell with a = 24.567 (1) Å.

According to the formalism outlined in §2 the reflections can be separated into two sets. $F_{\rm av}$ represents reflections corresponding to the small cell with $a \simeq 12.3$ Å, *i.e.* with all indices even. The remaining reflections can be treated as $F_{\rm dif}$. These weak reflections were included in the data set used for calculation of the difference electron density using the band-flipping algorithm. Out of 5037 independent superstructure reflections in the data set 1415 were classified as observed ($I > 3\sigma$) with $R_{\rm int} = 12.0\%$.[1]

The first notable difference from the expectation is that the data set contained a large number of reflections violating the *F*-centring. Out of 4358 reflections in the merged data set that are forbidden by the *F*-centring, 993 had significant intensity ($I > 3\sigma$), and 303 had $I > 20\sigma$. Thus, it is clear that the space group of the investigated sample cannot be the expected $Fm\overline{3}c$. Analysis of systematic absences suggested Laue group $m\overline{3}m$, space group $Pn\overline{3}n$.

The iteration using the band-flipping algorithm converged to a stable solution in all of 100 test runs, with 489 cycles per convergence on average. In order to address the problem of the symmetry we used the recently published symmetry-determination algorithm (Palatinus & van der Lee, 2008). This algorithm does not rely on the analysis of systematic absences, but analyses the electron density (the difference electron density in the current case) for the presence of symmetry operations compatible with the lattice parameters. Each symmetry operation is assigned a so-called symmetry agreement factor $\phi_{\rm sym}$. The space group can be derived from the list of symmetry operations with sufficiently low $\phi_{\rm sym}$. The algorithm yielded unambiguously and reproducibly space group $Pn\overline{3}$. The $\phi_{\rm sym}$ of symmetry operations belonging to $Pn\overline{3}$ was less than 10% indicating a very good match, while all other symmetry operations (including the diagonal *n*-glide suggested by the systematic absences) had $\phi_{\rm sym} \simeq 40\%$ or more, indicating quite a poor match.

The reconstructed difference electron density is shown in Fig. 1. As mentioned above, the chemical ordering of Si and Al is not easily seen in X-rays owing to the proximity of their atomic numbers. However, the Al—O bonding distance is 0.14 Å longer than the Si—O bonding distance, and thus the ordering can be indirectly inferred from the bond lengths. The differences in bond lengths, and consequently the distortion of the TO_4 tetrahedra (T = Al, Si), can be derived from the difference map. In Figs. 1(*a*) and 1(*b*) part of the reconstructed difference density is shown with an overlaid framework structure of zeolite *A*. Shifts of the atomic positions relative to the average structure are clearly demonstrated by the occurrence of pairs of positive and negative peaks. The distortion is realized by shifts of the T atoms and mostly three of the four oxygen atoms. One oxygen in each tetrahedron shows only a very small shift from its average position. If we focus only on the positive (yellow) peaks in the figure, we can see the AlO_4 tetrahedra in the difference map as more 'expanded' tetrahedra, while the SiO_4 tetrahedra are clearly 'shrunken'. The alternating pattern of the Si and Al tetrahedra breaks the $Pm\overline{3}m$ symmetry of the average structure, but is compatible with the $Fm\overline{3}c$ symmetry. However, the real positions of the maxima and minima in the difference map break even the $Fm\overline{3}c$ symmetry beyond any doubt. Two slightly differently distorted frameworks can be found in the subcells of the superstructure. Their alternated linking along ⟨100⟩ forms the $2 \times 2 \times 2$ superstructure ordering.

An attempt to solve the structure by standard charge flipping using the full data set does not lead to a reliable determination of the superstructure. The iteration converges with surprising difficulty. Only 49 out of 100 runs converged within 15 000 cycles. The difficulty was caused by the large number of missing strong reflections in the data set, as the 32 strongest reflections were missing because of saturation of the detector. However, even the converged runs did not provide any useful information about the superstructure. The symmetry analysis

[1] The complete reflection list including the reflections with all indices even has been deposited as supplementary material and is available from the IUCr electronic archives (Reference: SH5114). Services for accessing these data are described at the back of the journal.

yielded low symmetry-agreement factors for all symmetry operations of the $Pm\bar{3}m$ symmetry. For example, the fourfold axis 4_x, which is not present in the superstructure, had on average $\phi_{sym} \simeq 10\%$, while the diagonal threefold axis yielded $\phi_{sym} \simeq 13\%$. The proximity of ϕ_{sym} of false and true symmetry operations means that the phases of the superstructure reflections are essentially random, and do not allow the determination of the superstructure from the complete data set.

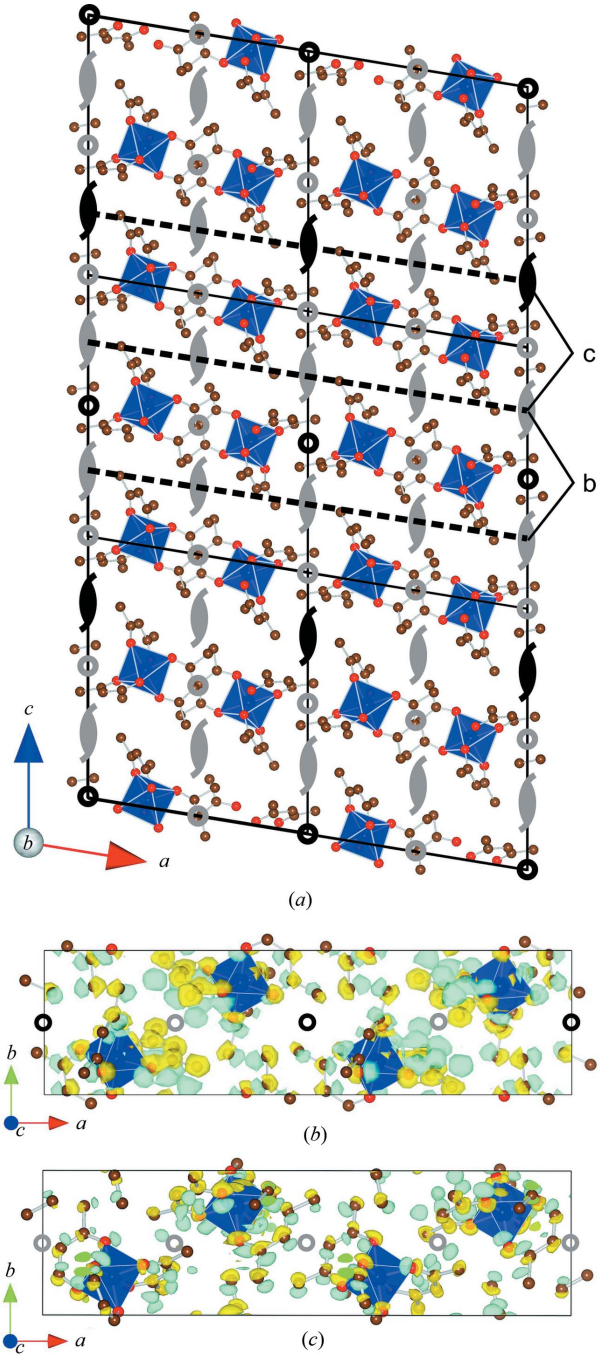

Figure 2
(*a*) One unit cell of the low-temperature structure of $Cr^{III}(acac)_3$ with highlighted positions of the symmetry operations of the room-temperature structure. Black symbols represent the true symmetry operations of the low-temperature structure, while the grey symbols are pseudosymmetry elements. Dashed lines and letters 'b' and 'c' show the slabs of the structure shown in (*b*) and (*c*). (*b*), (*c*) View of two slabs of the structure along [001] with superimposed difference density shown as isosurfaces. The true (black circle) and false (grey circle) inversion centres are easily recognized. Positive density is shown in yellow, negative in turquoise.

It is not the purpose of this work to reopen the discussion about the true symmetry of the Na-*A* zeolite. We believe that it has become clear in the meantime that the exact symmetry depends critically on the preparation conditions and sample history. We know neither the exact sample preparation procedure, nor the exact Si:Al ratio of the sample. Moreover, the fact that the sample was measured at 100 K can have an influence on the symmetry. It is clear, however, that the presented method is a powerful tool that can be used to address such complicated problems of symmetry, and yield more convincing results than conventional approaches.

3.2. Chromium triacetylacetonate

The structure of chromium triacetylacetonate $Cr(C_5H_7O_2)_3$ [$Cr^{III}(acac)_3$] (von Chrzanowski *et al.*, 2007) is formed by Cr atoms octahedrally coordinated by six O atoms belonging to three acetylacetonate molecules. The low-temperature structure is a sixfold superstructure of the room-temperature structure. Both structures have the space group $P2_1/c$, and their unit cells are related by the matrix $\mathbf{S} = (2\,0\,0|0\,1\,0|0\,0\,3)$. von Chrzanowski *et al.* (2007) point out that the transformation of the room-temperature structure to the low-temperature superstructure can lead to different structures, which differ by the choice of the position of the inversion centre (Fig. 2*a*). Four symmetry-independent choices of the inversion centre are possible. They are equivalent to four possible origin shifts of the supercell. If a wrong choice is made, the inversion centre is placed at a pseudosymmetric position. The least-squares refinement procedure will not converge from the wrong setting to the correct one. The wrong structure can be refined to reasonable *R* values, with just a few suspicious anisotropic displacement parameters which could be, with a lack of critical crystallographic thinking, attributed to disorder. It is notable that several of the commonly used structure solution programs suggest the wrong choice of the origin when the structure of chromium triacetylacetonate is solved *ab initio* (von Chrzanowski *et al.*, 2007).

The data were collected on a laboratory X-ray Nonius KappaCCD diffractometer with Mo $K\alpha$ radiation. The average intensity of the superstructure reflections (all reflections for which $h \neq 2n$ or $l \neq 3n$) is only 3.2% of the average intensity of the main reflections. It is thus not surprising that it is not easy to distinguish the correct from the wrong choice of the inversion centre in the complete structure (Fig. 2*a*), and that the phasing procedure may fail in finding the correct phases of the superstructure reflections. One hundred runs of *SUPERFLIP* with standard settings and with all reflections included in the data set were performed and analysed. All runs converged with a mean of 157 cycles per convergence. Out of these 100 runs the correct origin was located in 90 cases. In the other ten cases the origin was placed incorrectly in the point

Table 1
Symmetry agreement factors ϕ_{sym} for the four possible origin choices of low-temperature chromium triacetylacetonate.

The statistics were obtained from 92 converged runs.

Origin shift	Mean	Minimum	Maximum
Standard charge flipping on all reflections			
0 0 0	2.96	1.24	7.24
0 0 $\frac{1}{6}$	12.94	7.28	20.12
$\frac{1}{4}$ 0 0	21.44	9.54	23.69
$\frac{1}{4}$ 0 $\frac{1}{6}$	6.60	2.70	10.77
Band flipping on superstructure reflections			
0 0 0	12.17	9.96	15.87
0 0 $\frac{1}{6}$	90.07	52.41	124.75
$\frac{1}{4}$ 0 0	146.07	133.78	161.66
$\frac{1}{4}$ 0 $\frac{1}{6}$	39.40	22.82	61.84

($\frac{1}{4}$, 0, $\frac{1}{6}$) of the correct structure. The degree of pseudosymmetry for various origins can be well described by their overall symmetry agreement factors ϕ_{sym}. This factor is an overall measure of the match of all symmetry operations for the particular choice of origin (Palatinus & van der Lee, 2008). Table 1 summarizes the agreement factors obtained for the four possible symmetry-independent choices of origin. It reveals that especially the point ($\frac{1}{4}$, 0, $\frac{1}{6}$) shows a particularly high pseudosymmetry. Its ϕ_{sym} is significantly larger on average than the ϕ_{sym} of the correct origin, but the intervals of observed ϕ_{sym} overlap for these two choices of origin. It can be concluded that the standard charge flipping solves the structure correctly in most cases, but fails occasionally, as the distinction between the correct and incorrect origin on the basis of ϕ_{sym} is difficult.

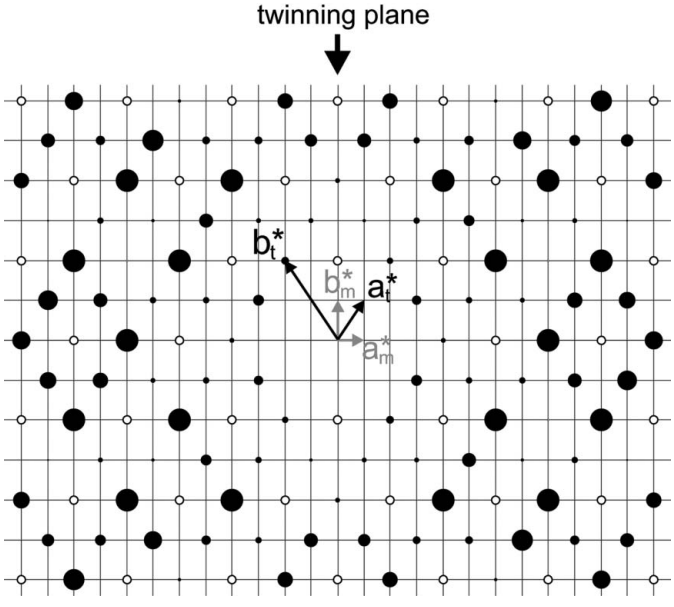

Figure 3
Intensity distribution in the *hk*0 plane of the diffraction pattern of $Eu_2Si_2O_7$. Solid circles represent observed reflections, empty circles show reflections with insignificant intensity. The basic vectors of the incorrect monoclinic reciprocal base (subscript 'm') and one of the two orientations of the correct triclinic base (subscript 't') are outlined with grey and black arrows, respectively.

The difference density can be solved easily using band flipping followed by five cycles of band elimination. An inspection of the reconstructed difference density leaves no doubt about the correct placement of the inversion centre (Figs. 2*b*, 2*c*). The main shifts of the molecules can be directly seen in the difference density as close-lying pairs of positive and negative peaks. Out of 100 runs 92 converged successfully with, on average, 526 cycles per run. The remaining eight converged to partial solutions of insufficient quality. The symmetry agreement factors obtained in the 92 successful runs are listed in Table 1. The ϕ_{sym} of the correct solution is clearly the lowest, and there is no overlap between the interval of ϕ_{sym} for the correct and incorrect origin choices. The band-flipping calculation using only the superstructure reflections revealed the correct origin in all 92 converged runs. Note that ϕ_{sym} of 100 corresponds to a random density. The values of ϕ_{sym} exceeding 100 thus indicate a certain degree of antisymmetry.

3.3. Dieuropium disilicate

Crystals of dieuropium disilicate were obtained in a small quantity as a by-product of a reaction of Eu_2O_3 with $Sb_4O_5Cl_2$ in evacuated quartz ampoules at 1123 K. A small single crystal was measured on a Stoe IPDS 1 single-crystal diffractometer with Mo $K\alpha$ radiation. All reflections could be indexed with a *C*-centred monoclinic unit cell with cell dimensions $a = 22.845$, $b = 14.358$, $c = 6.680$ Å and $\beta = 91.32^\circ$. However, the structure could not be solved from the diffraction data. An inspection of the distribution of the intensities in the *hk*0 plane (Fig. 3) revealed immediately that the crystal is a twin by reticular pseudomerohedry that can be described by a triclinic unit cell with dimensions $a = 13.491$, $b = 6.746$, $c = 6.680$ Å, $\alpha = 88.89$, $\beta = 91.11$ and $\gamma = 115.70^\circ$. The twinning matrix **T** that transforms the reflection indices of the second twin domain to the reciprocal basis of the first twin domain (*i.e.* $\mathbf{h}_1 = \mathbf{h}_2\mathbf{T}$) is

$$\mathbf{T} = \begin{pmatrix} 0 & -\frac{1}{2} & 0 \\ -2 & 0 & 0 \\ 0 & 0 & 1 \end{pmatrix}. \qquad (9)$$

It follows from the twinning matrix that all reflections with the index *h* even will transform to integer indices and will thus overlap with a reflection of the second twin domain, while all reflections with the index *h* odd will remain separated. Using the separated reflections as F_{dif}, *i.e.* setting the superstructure matrix **S** – see §2 – to (2 0 0|0 1 0|0 0 1), allows us to solve the difference density between the true density and a superposition density obtained by overlapping two halves of the unit cell along **a**.[2]

The difference map could be solved with the band-flipping method. The iteration always quickly converged to a solution,

[2] The reflection list indexed in the triclinic cell and containing all reflections that can be indexed in one twin domain has been deposited as supplementary material and is available from the IUCr electronic archives (Reference: SH5114). Services for accessing these data are described at the back of the journal.

with an average of 214 cycles per convergence. A typical difference map is shown in Fig. 4(*a*) together with an overlaid structure. The interpretation of the density is quite straightforward. In contrast to the superstructures, where the atoms of the individual subcells lie usually quite close, in the current case the two subcells (two halves of the unit cell along **a**) do not show any significant overlap, and therefore the positive peaks in the difference density can be directly interpreted as positions of atoms.

We note that the structure of $Eu_2Si_2O_7$ can also be solved without resorting to the reconstruction of difference electron density. The simplest approach is to use all reflections that can be indexed by one of the twin domains, and to ignore the fact that part of the reflections contain a contribution from the other domain. The resulting electron density is shown in Fig. 4(*b*). It provides sufficient information for building an initial structure model, but the density is much more noisy and contains a lot of artifacts. Even when ignoring the Fourier artifacts lying close to Eu atoms, the density map contains four spurious peaks with density higher than the density at the position of O atoms. On the other hand, the difference density in Fig. 4(*a*) is clear and contains no spurious peaks. The increase of the quality of the reconstructions is significant, but not critical for the structure solution in this case. However, the improvement can be crucial in cases of more complex structures.

3.4. Modulated structure

Twinning is a frequent phenomenon occurring in modulated structures resulting from phase transitions. In many cases the twinning law brings main reflections onto other main reflections, but the satellites of each twin domain remain separated. In other cases a coexistence of a non-modulated and modulated phase is possible (Krueger *et al.*, 2009). If the modulation is strong, the inability to obtain accurately the intensity of the main reflections can hinder the structure solution. And even if all intensities are available and twinning is not a problem, it can sometimes be difficult to see clearly the modulation if all reflections are used as an input for charge flipping. Charge flipping does not make use of the concept of point-like atoms, and it can thus be used for *ab initio* reconstructions of modulated structures directly in superspace (Palatinus, 2004), and the same concept can be used for reconstruction of the difference between the modulated and average density using the band-flipping approach. For the illustration of the application we show here the solution of the modulation of chromium diphosphate. This structure does not exhibit twinning, nor have there been any problems with the collection of the complete diffraction pattern. We choose this structure just as an example, because most cases where the application of this method would be of real interest contain additional complications that make it unsuitable for a brief presentation within the scope of this paper.

Chromium diphosphate $Cr_2P_2O_7$ has an incommensurately modulated structure at room temperature (Palatinus *et al.*, 2006), superspace group $C2/m(\alpha 0\gamma)0s$. The data were measured on a laboratory Oxford Diffraction CCD diffractometer using Mo $K\alpha$ radiation, and the structure was easily solved by the standard charge-flipping algorithm, and then refined using the computing system *JANA2006* (Petříček *et al.*, 2006). The atom positions are modulated with a variety of modulation functions, including crenel functions and sawtooth functions, *i.e.* linear functions with slope and point of

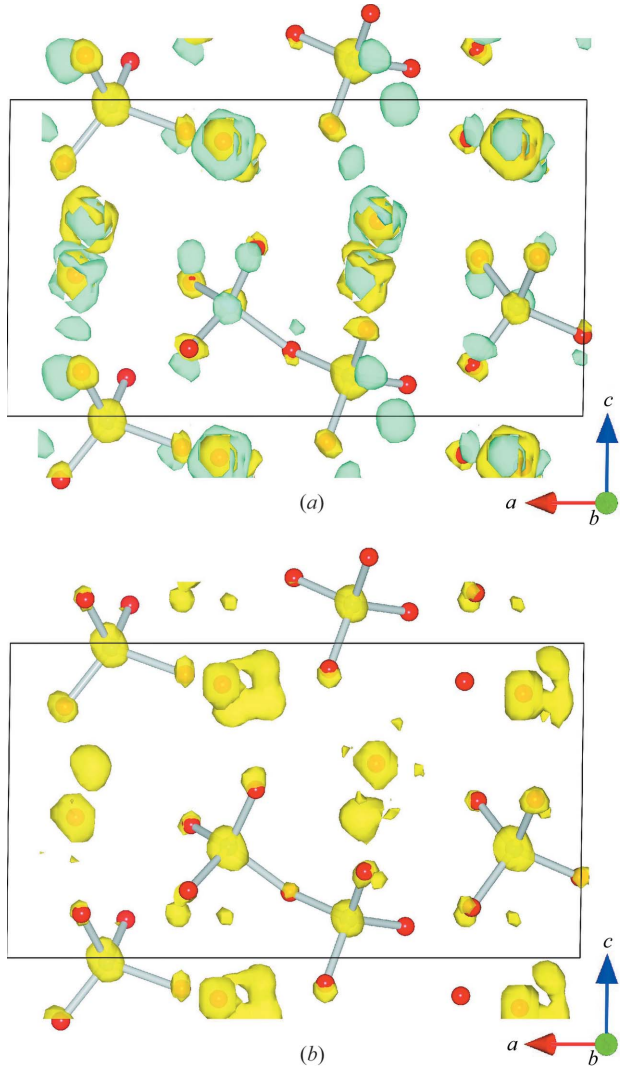

Figure 4
Structure of $Eu_2Si_2O_7$ projected along **c** with superimposed electron densities reconstructed by charge flipping. The structure is plotted as separate Eu atoms and SiO_4 tetrahedra connected by bond sticks. Only one half of the unit cell along **c** is shown for clarity. (*a*) Difference electron density reconstructed by band flipping from a data set with only odd *h* indices. (*b*) Total electron density reconstructed by the standard charge flipping on a full data set. Positive density is shown in yellow, negative in turquoise. Only positive density shown in (*b*). All density peaks in (*b*) without an associated atom are ghost peaks. The isosurfaces are drawn at 75% of the density of the smallest atomic peak. Note: the densities were treated with an algorithm for removing Fourier artifacts. This algorithm is implemented in the program *SUPERFLIP* as an experimental feature. It was inspired by the resolution bias correction algorithm (Altomare *et al.*, 2008). Without this treatment the features in the image would be obscured by the Fourier artifacts around the Eu atoms. The application or not of the treatment has no impact on the conclusions that can be drawn from the maps.

discontinuity. If the main reflections are removed from the reflection list, the difference density between the true and the average structure can be reconstructed by the band-flipping algorithm. The convergence was rapid and reproducible in this case. Two two-dimensional sections through the four-dimensional electron density are shown in Fig. 5. The sections show positions of the chromium atom, and one of three independent oxygen atoms. Both total electron density (as calculated from the final structure model) and the *ab initio* reconstructed difference density are shown for comparison. It is obvious that the main features of the modulation can be clearly seen in the difference density. It is notable that the difference density at the position of the oxygen atom shows clearly the discontinuous nature of the modulation (Fig. 5*d*). This can be deduced from the abrupt switching of the positive difference density from left to right and back along x_4. Such a distinction between the harmonic and discontinuous modulation cannot be made from the total density (Fig. 5*c*).

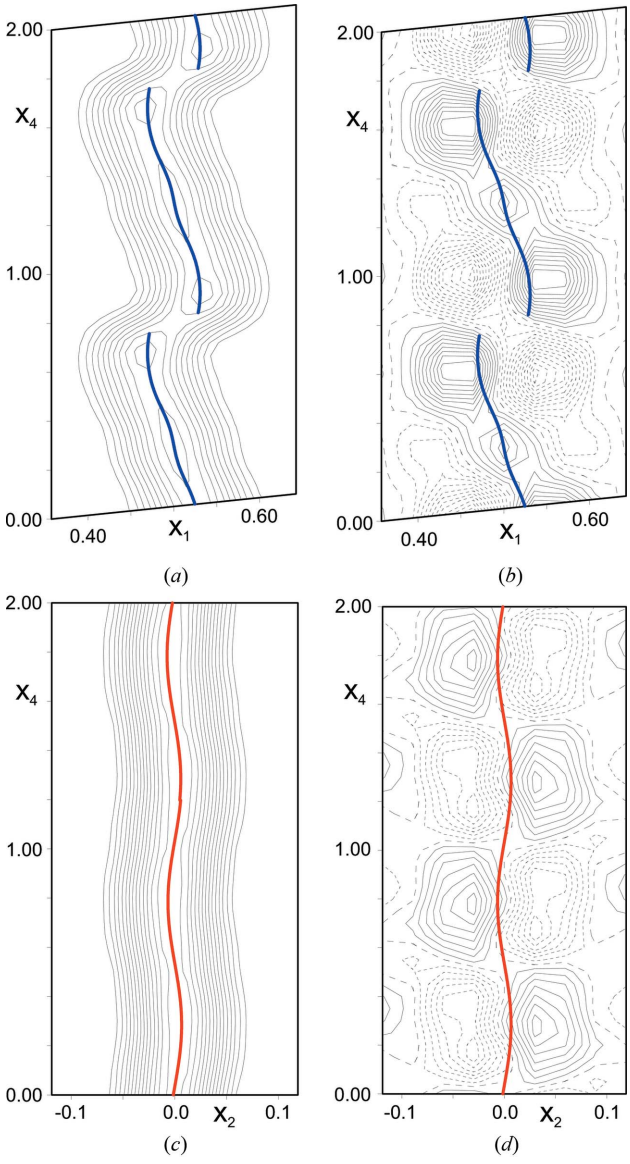

Figure 5
Sections through the superspace electron density of $Cr_2P_2O_7$. (*a*) x_1–x_4 section through the position of atom Cr showing the total density calculated from the final structure model. (*b*) The same section as in (*a*) through the *ab initio* determined difference density. (*c*) x_2–x_4 section through the position of atom O1 showing the total density calculated from the final structure model. (*d*) The same section as in (*c*) through the *ab initio* determined difference density. The thick lines in the sections show the refined modulation function. The contour interval in (*d*) is ten times smaller than in (*b*).

3.5. Quasicrystal superstructure

Structure solution methods like CF and LDE or their variants require periodic boundary conditions of the underlying structure, which are fulfilled for QCs in their higher-dimensional (*N*D) description. Diffraction patterns of QCs can be indexed with integer numbers based on a set of $3 + d$ independent basis vectors, where $N = 3 + d$ is the dimensionality of the periodic boundary condition. The atomic structure in the *N*D description consists of so-called occupation domains (ODs), which are geometric objects, only extended along the perpendicular-space dimensions $\mathbf{V}^{\perp}$. The three-dimensional physical space $\mathbf{V}^{\parallel}$ and the *d*D perpendicular space $\mathbf{V}^{\perp}$ are two orthogonal subspaces of the Euclidean embedding space $\mathbf{V} = \mathbf{V}^{\parallel} \otimes \mathbf{V}^{\perp}$. The reconstruction of the ODs in position, size, shape and occupation is the subject of the structure solution and refinement process of QCs.

It has been shown that the structure solution methods CF and LDE are successful in solving QCs (Takakura *et al.*, 2001; Katrych *et al.*, 2007). However, no structure solution for quasiperiodic superstructures is reported and iterative phase-retrieval algorithms or other structure solution methods can provide solutions for their average structure only. We show that the band-flipping variant of the CF algorithm is able to reconstruct the difference density from simulated diffraction data of a decagonal quasiperiodic superstructure. Decagonal QCs are structures with a periodic stacking of quasiperiodic layers with five- or tenfold rotational symmetry. Several superstructures have been found in decagonal quasiperiodic phases (for a comprehensive review see Steurer, 2004). They can be divided into superstructures along the periodic direction, within the quasiperiodic layers or as combinations of both. Yamamoto & Weber (1997) and Yamamoto *et al.* (2005) developed five-dimensional models for the quasiperiodic superstructures AlFeNi and AlCoNi (S1 phase) by introducing colour symmetry to explain the superstructure reflections in the diffraction pattern. According to these models, subdomains of the disc-like-shaped ODs are related by anti-symmetry operators, which transform one property to its inverse.

We modelled a fivefold decagonal superstructure based on colour symmetry. The superstructure has a lattice parameter a = 5.19 Å, which is $2\cos(\pi/10)$ times larger than the average structure with a lattice parameter of a_0 = 2.73 Å. The lattice parameter along the periodic direction for both structures is $c = c_0$ = 4.09 Å. We defined the basis vectors in the direct five-dimensional space by $\mathbf{d}_j = (2a/5^{1/2})[(c_j - 1)\mathbf{e}_1 + s_j\mathbf{e}_2 + (c_{2j} - 1)\mathbf{e}_3 + s_{2j}\mathbf{e}_4]$ with $j = 1, \ldots, 4$ and $\mathbf{d}_5 = c\mathbf{e}_5$, where $c_j = \cos(2\pi j/5)$ and $s_j = \sin(2\pi j/5)$. The vectors $\mathbf{e}_1$, $\mathbf{e}_2$ and

$\mathbf{e}_5$ are parallel-space unit vectors, and $\mathbf{e}_3$ and $\mathbf{e}_4$ are perpendicular-space unit vectors. The basis in reciprocal space is therefore defined by $\mathbf{d}_j^* = (a^*/5^{1/2})(c_j\mathbf{e}_1 + s_j\mathbf{e}_2 + c_{2j}\mathbf{e}_3 + s_{2j}\mathbf{e}_4)$ and $\mathbf{d}_5^* = c^*\mathbf{e}_5$ with $a^* = 1/a$ and $c^* = 1/c$. The model structure consists of two symmetry-independent pentagonally shaped ODs, where the OD *A* has a diameter of $2\tau a/[5(1+\tau^2)]^{1/2}$ [τ is the golden mean; $\tau = 2\cos(\pi/5) \simeq 1.61803\ldots$] and is located at (0, 2, −1, 1, 1.25)/5. The τ-times larger OD *B* is located at (0, 4, −2, 2, 1.25)/5 and fully occupied with Al. OD *A* is divided into several subdomains with different site-occupancy factors. An inner star is fully occupied with Co and the outer subdomains with Al. The Al-occupied subdomains in OD *A* were modelled with a site occupancy of 0.5 in the average structure, while in the superstructure two of these subdomains are related by a colour mirror plane. Therefore, the site-occupancy factor of one subdomain is increased by 0.5 and that of the colour-symmetry-related domain is reduced by the same value, or, in other words, one subdomain is fully occupied with Al and the other unoccupied (Fig. 6).

The colour space group of the superstructure is $P10_5/mc'm'$, where the ‘′’ denotes the antisymmetry operators. The average structure is described in the space group $P10_5/mmc$.

We calculated the diffraction data of the modelled phase by Fourier transform of the five-dimensional structure, applying an overall Debye–Waller factor in parallel space of 0.019 Å^2. The phasonic Debye–Waller factor, which describes random fluctuations along the perpendicular-space coordinates, was set to 0.020 Å^2. The calculated intensities were scaled so that the intensity of the strongest reflection except $F(\mathbf{0})$ is 10 000 counts. Normally distributed random numbers with a variance $\sigma^2 = I_{\rm calc}(\mathbf{h})$ were added to simulate noise in the counting statistic.

The lattice vectors in the reciprocal space defining the average structure and the superstructure are related by the transformation matrix S = (1 0 1 $\bar{1}$ 0|0 1 1 0 0|$\bar{1}$ 0 2 0 0|0 $\bar{1}$ 1 1 0|0 0 0 0 1). The determinant of the transformation matrix is 5 and, therefore, the superstructure is a fivefold superstructure of the basic structure. The superstructure reflections amount to approximately 75% of all reflections but contain only 2% of the integrated intensity of the data set. Even the strongest superstructure reflection has a signal-to-noise ratio of $7/7^{1/2} < 3$.

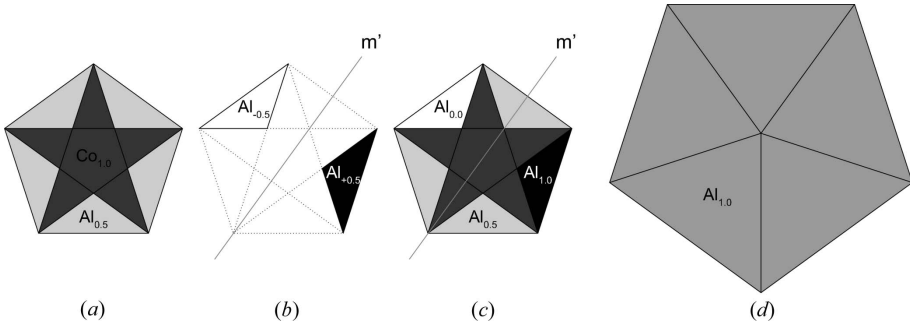

Figure 6
Model of the superstructure in a decagonal QC. Modelled symmetry independent OD *A* of (*a*) the average structure, (*b*) the difference structure, (*c*) the superstructure located at (0, 2, −1, 1, 1.25)/5 and (*d*) OD *B* located at (0, 4, −2, 2, 1.25)/5. The subdomains coloured in black and white represent the parts of the OD which are related by the colour symmetry operator ‘m’. Dark grey indicates the occupation of subdomains by cobalt and light grey indicates different occupation by aluminium, which is unaffected by the colour symmetry.

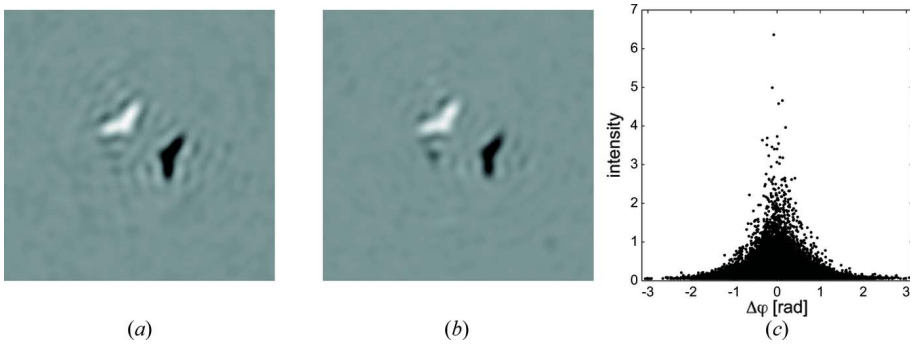

Figure 7
Reconstructed difference map of the OD *A* at (0, 2, −1, 1, 1.25)/5 from (*a*) the correct phases and (*b*) a single band-flipping run with 20 subsequent band-elimination cycles (white corresponds to negative densities and black to positive densities; densities about zero are grey). (*c*) The quality of the reconstructed difference map is represented in the phase difference between the correct and the retrieved phases of superstructure reflections.

The superstructure was solved using the band-flipping variant of the CF algorithm applied to the diffraction data containing only superstructure reflections. To reduce noise in the resulting electron-density (ED) map, five subsequent band-elimination cycles were performed. We handled the diffraction data in the Laue group $\bar{1}$ and no symmetry averaging was performed. Fig. 7 shows the calculated difference map of the OD *A* located at (0, 2, −1, 1, 1.25)/5. The subdomains corresponding to the superstructure were reconstructed. The absolute density values of both subdomains are similar and the colour symmetry, anti-symmetric mirror planes in this case, is properly recovered.

Since we were using simulated diffraction data, a comparison between the reconstructed and the true phases is possible. Therefore, the reconstructed ED was shifted to the same origin as the reference ED. The phase difference $\Delta\varphi = \varphi_{\rm true} - \varphi_{\rm retrieved}$ was used as a figure of merit of the structure solution (Fig. 7*c*). The distribution is typical for successful CF and LDE solutions (Fleischer *et al.*, 2010). Strong reflections were retrieved with small phase errors and weak reflections with an almost random phase.

4. Discussion

The previous section demonstrates, using several examples, the applicability of the method to various crystallographic problems. The ability to reconstruct structure information from only a partial set of reflections is clearly a powerful alternative tool for some problems. The purpose of this work is to describe the method and to demonstrate its usefulness, but not to provide a systematic account of its properties and limitations. This will require gathering more experience with a wider variety of test cases. However, already the limited list of examples presented in this paper allows for some generalizations.

The only critical parameter of the charge-flipping iteration is the flipping parameter δ. The selection of its optimum value has been discussed several times for the standard charge-flipping algorithm (Oszlányi & Sütő, 2004, 2008; Pereboom, 2007; Dumas & van der Lee, 2008), but never for the band-flipping algorithm except for the qualitative note in Oszlányi & Sütő (2007) that the useful interval for δ is narrower for band flipping than for standard charge flipping under otherwise similar conditions. We can confirm this observation. The standard charge-flipping algorithm is relatively tolerant to changes in δ up to 20% or even more, with typical values of δ for small molecules around 1.1σ (Pereboom, 2007; Oszlányi & Sütő, 2008; σ is the standard deviation of the density values). On the other hand, for the band-flipping algorithm we observed an increased sensitivity to δ. As an example, for the quasicrystal superstructure the optimum δ was found to be 1.4σ, and the values outside the interval 1.35–1.60σ already yielded no solution. The increased value of δ compared to standard charge flipping with positive densities could be explained by the increased sensitivity of the iteration to traps. The possible traps occurring in densities without positivity constraints were discussed by Oszlányi & Sütő (2007). Increased δ results in an increased perturbation of the density, and thus in an increased ability to escape the traps in the iteration path. However, this hypothesis is just a qualitative explanation and cannot be used for predictions. We cannot but conclude that despite the increasing popularity of charge flipping and a growing body of work on the method the behaviour of its fundamental parameter is still relatively poorly understood.

Once the difference density is reconstructed, it has to be interpreted to obtain the desired structural information. A qualitative interpretation of the difference densities is usually possible, and has been demonstrated in the examples above, but a quantitative interpretation is often difficult or impossible. Probably the most serious difficulty is that if a pair of a positive and negative peak is formed owing to the displacement of an atom from its average position, then the amplitude of this displacement cannot be accurately inferred from the position of the difference peaks. It was nicely demonstrated by Rius *et al.* (1996) that for small-to-moderate displacements (up to $\simeq 50\%$ of the half-width of the atomic peak) the position of the difference peaks is essentially independent of the displacement, and it is only the height of the peak that changes. However, the peak height alone cannot be used for quantitative analysis either, unless the average density is known on the same absolute scale. In reality the best way to obtain quantitative information about atomic positions is to add the difference and average densities, and analyse the sum for the peak positions. If the average density is available on the same scale as the difference density, then this approach can be beneficial, but if the average density is not available, then there is no easy way to quantify the atomic shifts other than by performing the full structure refinement. A similar problem concerns the occupational ordering. As an example, an increased occupancy of one position in the supercell results in a positive peak in the difference density, but the height of the peak has no relationship to the absolute change of occupancy, unless the intensities are known on an absolute scale. This is, however, usually not the case. Despite the limited possibility of extracting quantitative information from difference densities, if the average structure is not available, the difference density can still provide a lot of qualitative or semi-quantitative information about the crystal structure. Particularly useful is the decreased sensitivity of the difference structure to effects of pseudosymmetry, and consequently the possibility of unambiguously determining the true space group of the superstructure.

5. Conclusions

The method of *ab initio* reconstruction of difference electron densities from diffracted intensities of the superstructure reflections has been demonstrated to be a general and efficient approach to deal with several types of superstructures. The main advantages of this approach are that it allows one to overcome pseudosymmetry effects, it allows for a more reliable determination of the true symmetry of the superstructures, and it provides structure information in cases when a subset of reflection intensities is not available, for example because of the overlap of multiple twin domains. The method has also been shown to be applicable to solution of structures twinned by reticular pseudomerohedry, to modulations in incommensurately modulated structures from only the satellite reflections, and for elucidating superstructures in quasicrystals.

We thank Norman Schlosser, University of Siegen, for providing the unpublished data of dieuropium disilicate. FF, TW and WS gratefully acknowledge the support of the Swiss National Foundation under grant No. 200020-121568.

References

Adams, J. M. & Haselden, D. A. (1982). *J. Chem. Soc. Chem. Commun.* pp. 822–823.
Altomare, A., Cuocci, C., Giacovazzo, C., Kamel, G. S., Moliterni, A. & Rizzi, R. (2008). *Acta Cryst.* A**64**, 326–336.
Baerlocher, Ch. & McCusker, L. (2010). *Database of zeolite structures*, http://www.iza-structure.org/databases/.
Beurskens, P. T. & Bosman, W. P. (1982). *Z. Kristallogr.* **159**, 139–140.

Beurskens, P. T. *et al.* (1990). *The DIRDIF90 Program System*. University of Nijmegen, The Netherlands.
Böhme, R. (1982). *Acta Cryst.* A**38**, 318–326.
Buerger, M. J. (1954). *Proc. Natl Acad. Sci. USA*, **40**, 125–128.
Bursil, L. A., Lodge, E. A., Thomas, J. M. & Cheetham, A. K. (1981). *J. Phys. Chem.* **85**, 2409–2421.
Charnel, J. F. (1971). *J. Cryst. Growth*, **8**, 291–294.
Chrzanowski, L. S. von, Lutz, M. & Spek, A. L. (2007). *Acta Cryst.* C**63**, m377–m382.
Dumas, C. & van der Lee, A. (2008). *Acta Cryst.* D**64**, 864–873.
Fleischer, F., Weber, T., Deloudi, S., Palatinus, L. & Steurer, W. (2010). *J. Appl. Cryst.* **43**, 89–100.
Gramlich-Meier, R. & Gramlich, V. (1982). *Acta Cryst.* A**38**, 821–825.
Hauptman, H. & Karle, J. (1959). *Acta Cryst.* **12**, 846–850.
Janssen, T., Chapuis, G. & de Boissieu, M. (2007). *Aperiodic Crystals.* New York: Oxford University Press.
Katrych, S., Weber, T., Kobas, M., Massuger, L., Palatinus, L., Chapuis, G. & Steurer, W. (2007). *J. Alloys Compd.* **428**, 164–172.
Krueger, H., Kahlenberg, V., Petricek, V., Phillipp, F. & Wertl, W. (2009). *J. Solid State Chem.* **182**, 1515–1523.
Lippmaa, E., Magi, M., Samoson, A., Tarmak, M. & Engelbardt, G. (1981). *J. Am. Chem. Soc.* **103**, 4992–4996.
Momma, K. & Izumi, F. (2008). *J. Appl. Cryst.* **41**, 653–658.
Nespolo, M. & Ferraris, G. (2004). *Acta Cryst.* A**60**, 89–95.
Oszlányi, G. & Sütő, A. (2004). *Acta Cryst.* A**60**, 134–141.
Oszlányi, G. & Sütő, A. (2005). *Acta Cryst.* A**61**, 147–152.
Oszlányi, G. & Sütő, A. (2007). *Acta Cryst.* A**63**, 156–163.
Oszlányi, G. & Sütő, A. (2008). *Acta Cryst.* A**64**, 123–134.
Oszlányi, G., Sütö, A., Czugler, M. & Pŕkányi, L. (2006). *J. Am. Chem. Soc.* **128**, 8392–8393.
Palatinus, L. (2004). *Acta Cryst.* A**60**, 604–610.
Palatinus, L. & Chapuis, G. (2007). *J. Appl. Cryst.* **40**, 786–790.
Palatinus, L., Dušek, M., Glaum, R. & El Bali, B. (2006). *Acta Cryst.* B**62**, 556–566.
Palatinus, L. & van der Lee, A. (2008). *J. Appl. Cryst.* **41**, 975–984.
Pereboom, R. (2007). *Charge flipping: Étude du paramètre δ.* Diploma Thesis École Polytechnique Fédérale de Lausanne, Switzerland.
Petříček, V., Dušek, M. & Palatinus, L. (2006). *The crystallographic computing system JANA2006*. Institute of Physics, Prague, Czech Republic.
Rius, J., Crespi, A. & Torrelles, X. (2007). *Acta Cryst.* A**63**, 131–134.
Rius, J. & Frontera, C. (2008). *Acta Cryst.* A**64**, 670–674.
Rius, J., Miravitlles, C. & Allmann, R. (1996). *Acta Cryst.* A**52**, 634–639.
Shiono, M. & Woolfson, M. M. (1992). *Acta Cryst.* A**48**, 451–456.
Smaalen, S. van (2007). *Incommensurate Crystallography.* New York: Oxford University Press.
Smith, J. V. & Pluth, J. J. (1981). *Nature* (*London*), **291**, 265.
Steurer, W. (2004). *Z. Kristallogr.* **219**, 391–446.
Takakura, H., Shiono, M., Sato, T. J., Yamamoto, A. & Tsai, A. P. (2001). *Phys. Rev. Lett.* **86**, 236–239.
Takéuchi, Y. (1972). *Z. Kristallogr.* **135**, 120–136.
Yamamoto, A., Takakura, H. & Abe, E. (2005). *Phys. Rev. B*, **72**, 144202.
Yamamoto, A. & Weber, S. (1997). *Phys. Rev. Lett.* **79**, 861–864.